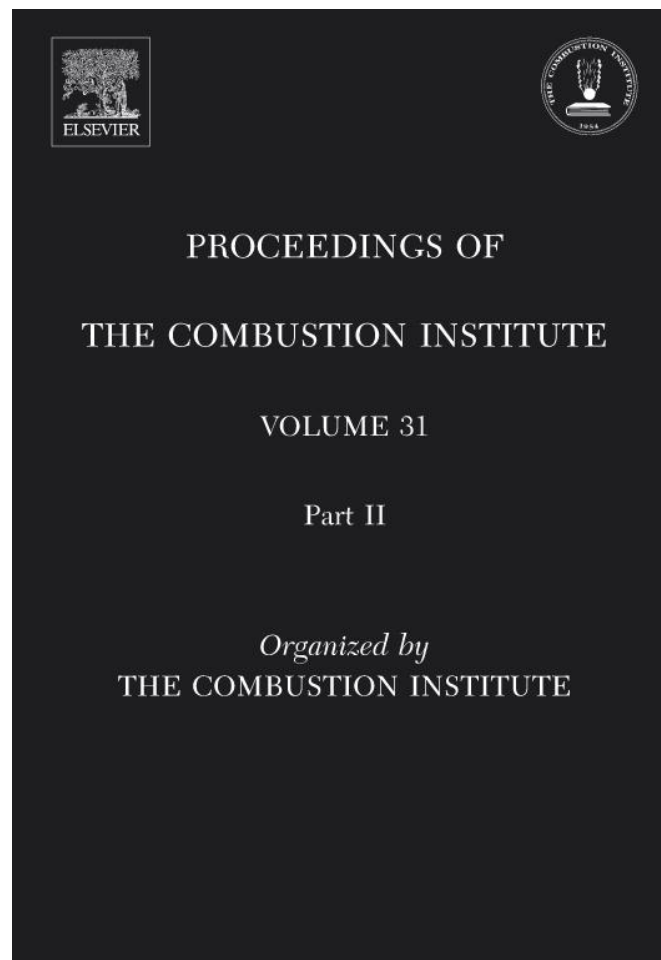


Provided for non-commercial research and educational use only.
Not for reproduction or distribution or commercial use.



This article was originally published in a journal published by Elsevier, and the attached copy is provided by Elsevier for the author's benefit and for the benefit of the author's institution, for non-commercial research and educational use including without limitation use in instruction at your institution, sending it to specific colleagues that you know, and providing a copy to your institution's administrator.

All other uses, reproduction and distribution, including without limitation commercial reprints, selling or licensing copies or access, or posting on open internet sites, your personal or institution's website or repository, are prohibited. For exceptions, permission may be sought for such use through Elsevier's permissions site at:

<http://www.elsevier.com/locate/permissionusematerial>



ELSEVIER

Available online at www.sciencedirect.com

ScienceDirect

Proceedings of the Combustion Institute 31 (2007) 2421–2428

Proceedings
of the
Combustion
Institute

www.elsevier.com/locate/proci

Shock wave and detonation propagation through U-bend tubes

S.M. Frolov ^{*}, V.S. Aksenov, I.O. Shamshin

N. Semenov Institute of Chemical Physics, Russian Academy of Sciences, 4, Kosigin street, Moscow 119991, Russia

Abstract

The objective of the research outlined in this paper is to provide experimental and computational data on initiation, propagation, and stability of gaseous fuel–air detonations in tubes with U-bends implying their use for design optimization of pulse detonation engines (PDEs). The experimental results with the U-bends of two curvatures indicate that, on the one hand, the U-bend of the tube promotes the shock-induced detonation initiation. On the other hand, the detonation wave propagating through the U-bend is subjected to complete decay or temporary attenuation followed by the complete recovery in the straight tube section downstream from the U-bend. Numerical simulation of the process reveals some salient features of transient phenomena in U-tubes.

© 2006 Published by Elsevier Inc. on behalf of The Combustion Institute.

Keywords: Gaseous detonation; Detonation initiation; Tube with U-bend; Shock-to-detonation transition

1. Introduction

Tube bends and coils are the elements, which can be used for elongating the detonation tubes of PDEs to ensure reliable deflagration-to-detonation transition (DDT) or shock-to-detonation transition (SDT). Surprisingly little work has been done on the DDT, SDT, and detonation diffraction in such elements (see [1–3] and references therein). Our recent research on a liquid-fueled air-breathing PDE [4–6] has unequivocally demonstrated that tube coils do promote DDT efficiently. It is anticipated that depending on the tube diameter, U-bend curvature, and the characteristic lengths of tube segments attached to the U-bends, different diffractions of initiating shock waves and

developed detonations can result in various transient phenomena leading to SDT or failure of a developed detonation.

The objective of the research outlined in this paper is to provide experimental and computational data on gaseous fuel–air detonation waves (DW) and reactive shock waves (SW) propagating in tubes with U-bends. Such data will be used for deriving theoretical criteria to evaluate detonation initiation and stability conditions in terms of tube diameter, U-bend curvature, and characteristic lengths of tube segments between several U-bends.

2. Experimental setup

Figures 1a and b show the schematics of the experimental setups for the studies of detonation initiation and propagation in tubes with U-bends. The setups comprised the shock generator, pieces

^{*} Corresponding author. Fax: +7 095 6512191.

E-mail address: smfrol@chph.ras.ru (S.M. Frolov).

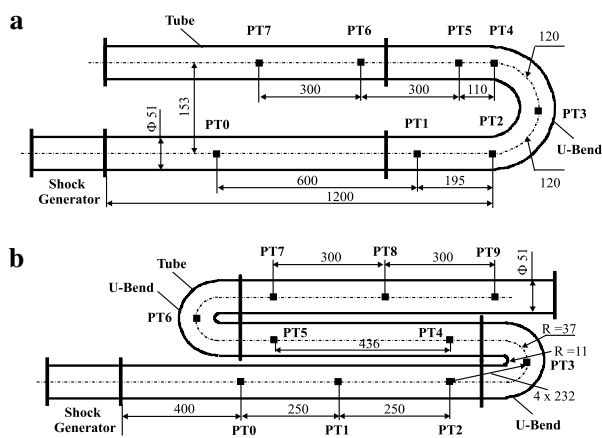


Fig. 1. Schematics of the experimental setups for the studies of detonation initiation and propagation in tubes with U-bends of different curvature: (a) 51 mm and (b) 11 mm.

of straight tube 51 mm in inner diameter, and U-bends made of the tube of the same diameter. The far end of the tube opposite to the shock generator was closed. The internal radii of the U-bends were equal to 51 mm (Fig. 1a) and 11 mm (Fig. 1b).

The shock generator was a combustion chamber 22 cm³ in volume equipped with a changeable nozzle of up to 14 mm in diameter closed with a bursting diaphragm. Before the run the combustion chamber was filled with a solid propellant (the mass up to 2.5 g). The propellant was ignited by an igniter 0.2 ± 0.02 g in mass. The maximal pressure in the chamber was 100 MPa. The strength of the SW formed depended on the nozzle diameter, diaphragm thickness, and thermodynamic parameters of combustion products in the shock generator.

Before each run, the detonation tube was evacuated and filled with the stoichiometric propane–air mixture at initial pressure of 0.1 MPa and initial temperature of 294 ± 2 K.

The measuring system included piezoelectric pressure transducers, photo-diodes, analog-to-digital converter, and a PC. The pressure transducers PT0, PT1, ..., PT9 were mounted along the tube as shown in Figs. 1a and b. The pressure transducer PT0 was used for triggering the measuring system.

The velocity of the SW was calculated using the formula $V = X/\Delta t$, where X is the length of the measuring segment and Δt is the time interval determined from the pressure records. The measuring segments PT0–PT1, PT1–PT2, etc. corresponded to the segments between pressure transducers PT0 and PT1, PT1 and PT2, etc., respectively. The error in determining X was ±0.5 mm which gave about 0.5% error for the shortest measuring segment (PT4–PT5 in Fig. 1a) 110 mm long. The time interval Δt was

determined at the half-amplitude levels of pressure transducer signals. Because of the finite dimensions of the transducer's sensitive element, the duration of the shock (and detonation) front registration was no less than 3 μs. The characteristic sampling time of each measuring channel was 1.2 μs, which allowed the resolution of the wave front with two to three samples. Thus the time interval Δt was determined with an uncertainty of ±2.4 μs. The detonation velocity in the stoichiometric propane–air mixture was at the level of 1800 m/s. The mean time interval taken for the DW to pass the shortest measuring segment was about 61 μs. Hence the maximal error in determining Δt was ±4%, and the corresponding error of determining the SW and DW velocity did not exceed 5%. The lengths of the measuring segments PT2–PT3 and PT3–PT4 in the U-bend of Fig. 1a were measured along the arc and were equal to 120 mm. In the U-bends of Fig. 1b, the corresponding lengths were measured along the straight lines connecting the pressure transducers and were equal to 232 mm.

3. Experimental results

Figures 2a and b show the shock wave velocities measured at different measuring segments of the setups of Figs. 1a and b, respectively. Shown in each figure are only five representative runs: Run 1 to Run 5. Note that all runs were well reproducible at similar initial conditions. Figures 3a–d show the pressure records registered by pressure transducers PT1–PT7 in Runs 2–5 of Fig. 2a.

In Run 1, the mean incident SW velocity at the entrance to the U-bend (segment PT1–PT2) was about 575 m/s. The velocity of the SW decreased gradually with the distance traveled, although in the U-bend it was nearly constant (~580 m/s).

In Run 2, the mean incident SW velocity at the entrance to the U-bend was somewhat higher (about 805 m/s) than in Run 1. Nevertheless the qualitative behavior of the SW was similar to that in Run 1 except for the indication of the secondary explosion (SE) on the record of PT6 at $t \approx 2200 \mu\text{s}$ (Fig. 3a). Also, at $t \approx 3400 \mu\text{s}$ one can see the reflected blast wave (RW) appearance on the record of PT6. This blast wave propagated upstream at a velocity of 1530–1740 m/s and resembled a DW. Note that in the straight tube of the same length neither a SE nor a reflected detonation-like wave were observed, other conditions being similar.

In Run 3, the incident SW velocity at the entrance to the U-bend was about 1083 m/s, i.e., higher than in Run 2. The shock wave traversed the U-bend at a nearly constant velocity of about 1060 m/s but suddenly accelerated to 1215 m/s at segment PT5–PT6 and to 2027 m/s at segment

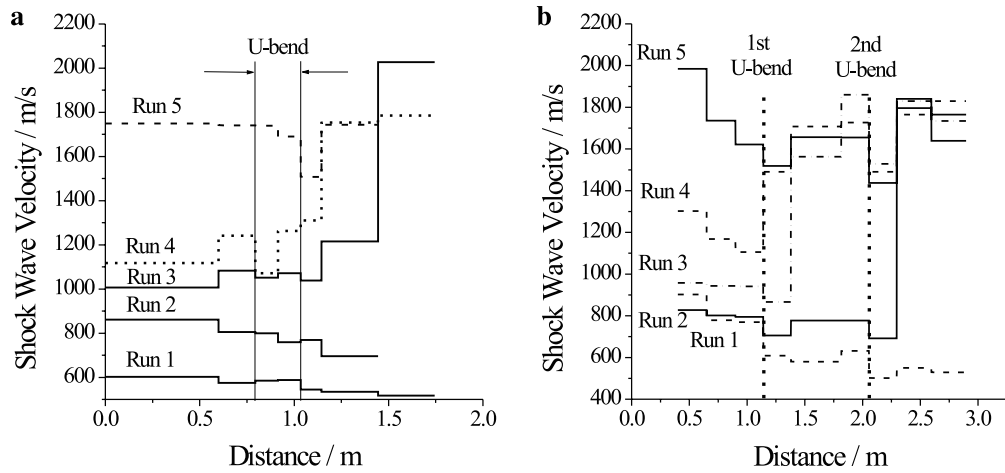


Fig. 2. Mean shock wave velocities at different measuring segments of the tubes with U-bends in five representative runs: (a) setup of Fig. 1a and (b) setup of Fig. 1b.

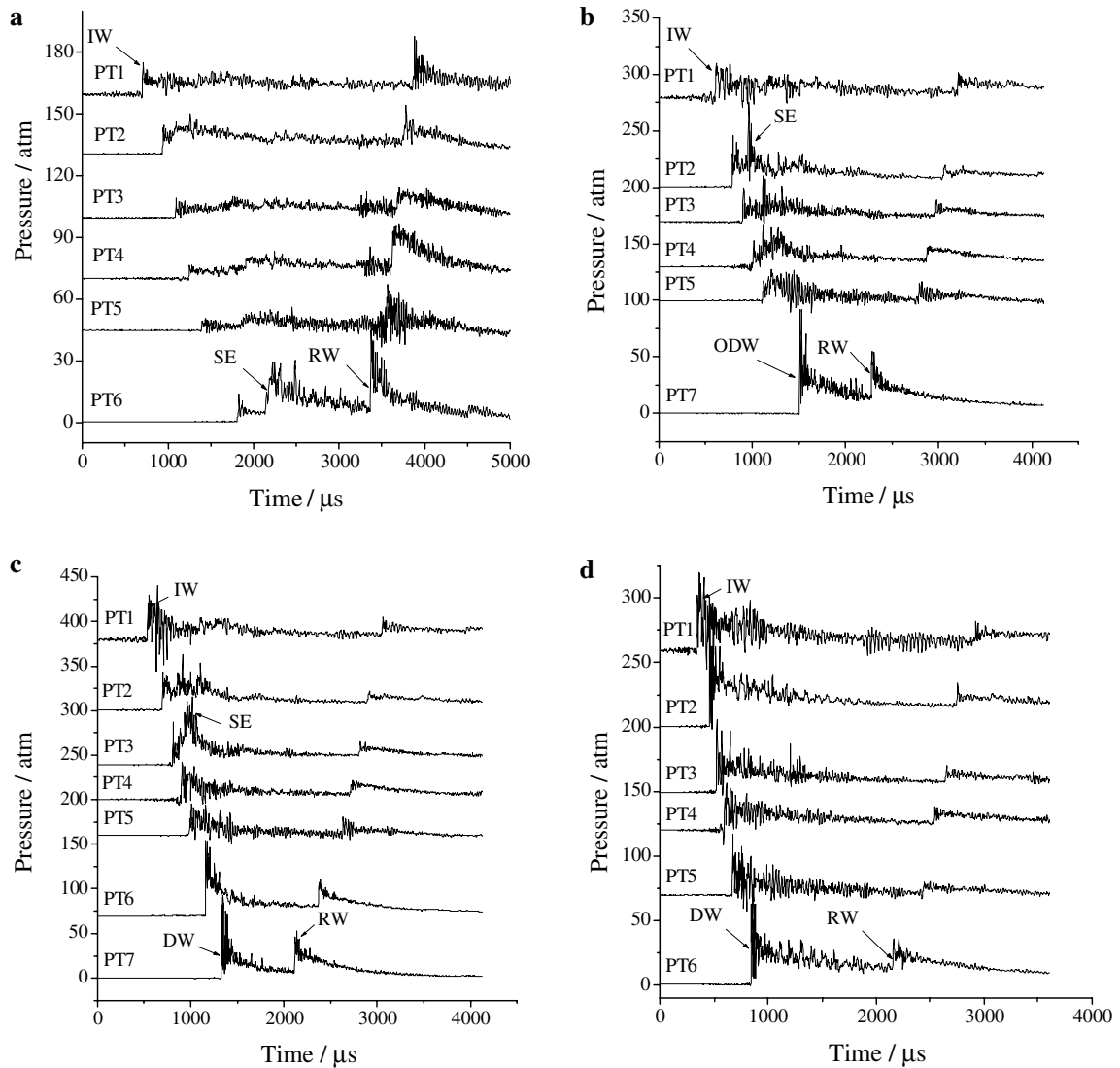


Fig. 3. Pressure records registered by transducers PT1–PT7 in four representative runs with different mean SW velocities at the entrance to a U-bend (measuring segment PT1–PT2 in Fig. 1a): (a) Run 2, $V = 805$ m/s; (b) Run 3, $V = 1083$ m/s; (c) Run 4, $V = 1242$ m/s; and (d) Run 5, $V = 1741$ m/s. IW = incident wave, RW = reflected wave.

PT6–PT7 (Fig. 2a). The latter value of the SW velocity corresponded to the overdriven DW (ODW). The reflected blast wave appearing at $t \approx 2300 \mu\text{s}$ on the record of PT7 (Fig. 3b) propagated upstream at the velocity varying from 1176 m/s at segment PT7–PT6 to 1481 m/s at PT3–PT2, and 1234 m/s at PT2–PT1. This wave propagated in partially reacted mixture as indicated by the records of PT2–PT5 exhibiting SE and pressure humps. Therefore its propagation velocity was lower than in Run 2.

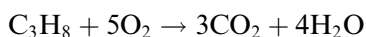
In Run 4, the mean incident SW velocity at the entrance to the U-bend was about 1242 m/s, i.e., higher than in Run 3. When entering the U-bend, the SW first decelerated to 1071 m/s at segment PT2–PT3 and then accelerated to 1263 m/s at segment PT3–PT4. This acceleration was most probably caused by the SE clearly seen on the record of PT3 in Fig. 3c. After passing the U-bend, the SW continued accelerating and transitioned to a detonation propagating at a velocity of 1750–1800 m/s at segments PT5–PT6 and PT6–PT7 (see Fig. 2a). The reflected blast wave appearing at $t \approx 2100 \mu\text{s}$ on the record of PT7 (Fig. 3c) propagated upstream at the velocity, which was nearly the same as in Run 3.

In Run 5, the mean incident SW velocity at the entrance to the U-bend, i.e., at segment PT1–PT2, was about 1741 m/s. At segment PT0–PT1 its velocity was about 1750 m/s. This propagation velocity was close to the Chapman–Jouguet (CJ) detonation velocity for the stoichiometric propane–air mixture at normal initial conditions. When traversing the U-bend, the DW decelerated to 1690 m/s at segment PT3–PT4 and then to 1507 m/s at segment PT4–PT5 after passing through the U-bend. However, it accelerated again to the initial propagation velocity of 1744 m/s at segment PT5–PT6 (Fig. 2a). The reflected blast wave appearing at $t \approx 2160 \mu\text{s}$ on the record of PT6 (see Fig. 3d) propagated upstream at the mean velocity varying from 1060 to 1170 m/s, which was somewhat higher than the sound speed in the detonation products ($\sim 1000 \text{ m/s}$).

In the setup of Fig. 1a, a SW entering the U-bend at a velocity exceeding 1100 m/s always transitioned to a detonation. In the setup of Fig. 2b, the lowest velocity of the SW entering the first U-bend had to exceed the value of about 800 m/s to ensure its transition to a detonation. Thus, on the one hand, the U-bends promoted SDT, the U-bends of larger curvature being more effective. On the other hand, the developed detonation wave propagating through the U-bend was subjected to temporary attenuation with a considerable velocity drop up to 15% in the setup of Fig. 1a and up to 20% in the setup of Fig. 1b. In some runs with the developed detonation in the setup of Fig. 1b, a complete decay of a DW was observed.

4. Computational approach

The mathematical model was based on the standard two-dimensional Euler equations, energy conservation equation with a chemical source term, and equation of chemical kinetics. The kinetics of propane oxidation was modeled by a single-stage overall reaction



The heat effect of the reaction entering the energy conservation equation was taken equal to 46.6 MJ/kg. The expression for a bimolecular reaction rate $w = k[\text{C}_3\text{H}_8][\text{O}_2]$ was used to calculate the rate of reaction, where k is the rate constant ($k = 7 \times 10^{14} p^{-0.2264} \exp(-E/RT) \text{ cm}^3 \text{ mol}^{-1} \text{ s}^{-1}$, T is the temperature, R is the gas constant, $E = 45460 \text{ kcal/mol}$ is the activation energy, and p is pressure in atm). The rate constant was obtained by fitting the calculated ignition delays with the experimental data [7,8] on ignition of the stoichiometric propane–air mixture behind reflected SW. In the fitting calculations, a zero-dimensional, constant-volume exothermal reaction kinetics was considered. Two definitions of the ignition delay were used: (i) as a time corresponding to the maximal rate of temperature rise and (ii) as a time corresponding to the characteristic ignition temperature $T = T_0 + RT_0^2/E$, where T_0 is the initial temperature. The resultant ignition delays obtained within both definitions were very close to each other.

For numerical solution of governing equations a method of splitting by physical processes [9] was used. At each time step, only convective fluxes and pressure work were taken into account at the first-stage. This stage of integration was solved by the second-order Godunov–Kogan method [10]. Mass, momentum, and energy fluxes through faces of a computational mesh were found from the exact solutions of the Riemann problem. At the second-stage, the chemical reaction was taken into account. Fully implicit method [11] was used for integrating the reaction kinetic equation. A more detailed description of the numerical procedure is available in [12].

5. Results of calculations

In the calculations, the same (but planar 2D) U-bend tube configurations as shown in Figs. 1a and b were studied. The tubes were initially filled with the stoichiometric propane–air mixture at $p = 0.1 \text{ MPa}$ and $T_0 = 298 \text{ K}$. A planar SW or DW was initiated by a short (10 mm long) tube section filled initially with the high-temperature (up to 2500 K) and high-pressure (up to 20 MPa) air simulating a shock generator of Fig. 1. The computational grid was uniform and contained 1600×400 square meshes with a size of 0.5 mm. The pressure histories at multiple

locations along the symmetry surface of the U-bend tube, as well as along its internal and external walls were stored during the calculations. Based on these numerical ‘pressure records,’ the corresponding propagation velocities of the lead shock front were calculated. In addition, 2D flow fields were stored to visualize the flow pattern.

Figure 4 shows the predicted SW velocities along the internal wall (a), symmetry surface (b), and external wall (c) of the tube of Fig. 1a. Dis-

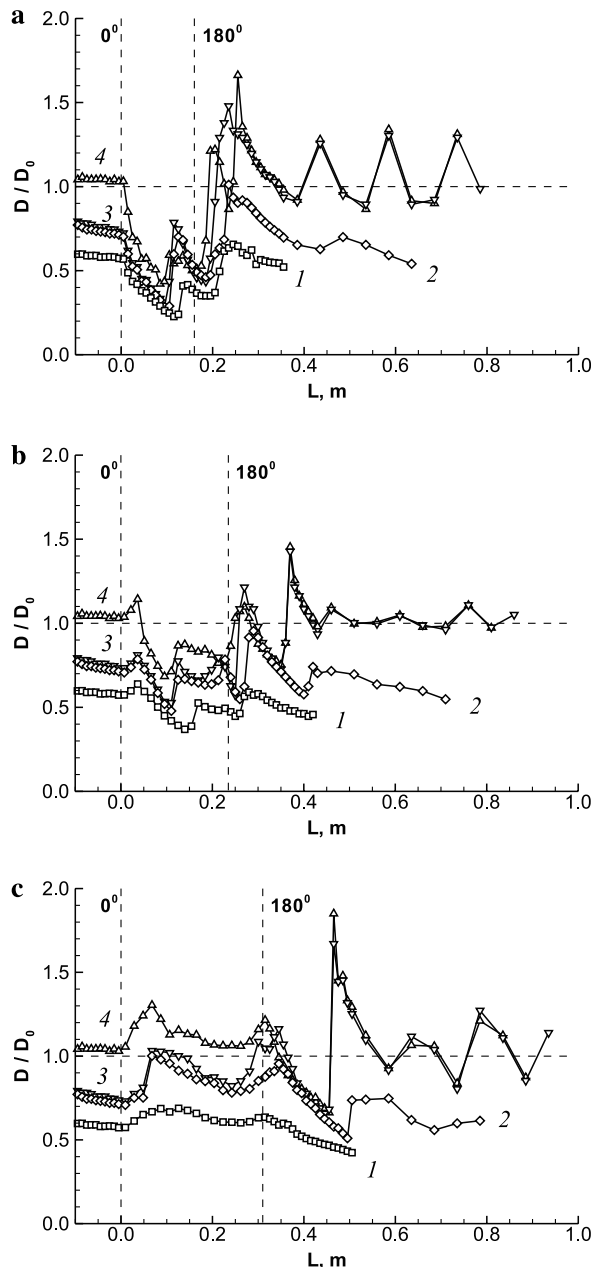


Fig. 4. Predicted normalized shock velocities along the internal wall (a), symmetry surface (b), and external wall (c) of the tube with U-bend. The origin of L -axis is located at the entrance to the U-bend. The regions between vertical dashed lines correspond to the U-bend section. Curves 1–4 correspond to different incident shock velocities: 1, $D/D_0 = 0.60$; 2, 0.73; 3, 0.75; and 4, 1.03.

tance L between two vertical dashed lines corresponds to the length of the U-bend segment measured along the corresponding surface. The SW velocity is normalized by the CJ detonation velocity D_0 , so that the horizontal dashed line $D/D_0 = 1$ corresponds to the CJ detonation velocity. Four cases with different velocities of the decaying reactive shock at the entrance to the U-bend were analyzed, namely $0.60D_0$ (curves 1 in Fig. 4), $0.73D_0$ (2), $0.75D_0$ (3), and $1.03D_0$ (4).

Entering the U-bend, the shock front started to interact with compressive and expansive surfaces. As a result, different portions of the front exhibited different behavior due to temporally and spatially shifted interaction with various compression and rarefaction waves and due to finite rate of chemical reaction. At the internal wall (Fig. 4a), the shock velocity decreased to the value between $0.2D_0$ (curve 1) and $0.4D_0$ (curve 4) nearly in the middle of the U-bend, which was caused by the rarefaction fan at the expansive surface. Subsequent velocity jump to about $0.4D_0$ (curve 1) and $0.8D_0$ (curve 4) at the internal wall was caused by interaction with a SW reflected from the external compressive wall. After passing through the U-bend, shock velocities at the internal wall exhibited a second jump also caused by interaction with a reflected SW.

At the symmetry surface (Fig. 4b) and external wall (Fig. 4c), the evolution of the lead shocks was somewhat different. Contrary to Fig. 4a, the lead shocks exhibited velocity increase on the entry to the U-bend. All other qualitative features were similar to those in Fig. 4a. Quantitatively, mean propagation velocities of the SW along the symmetry surface and external wall were higher than along the internal wall.

The results of Fig. 4 correspond with the experimental observations of Fig. 2a. Curves 1 in Fig. 4 correlate qualitatively with the results of Runs 1 and 2 in Fig. 2a with the decaying SW. Curves 4 correspond to the results of Run 5 with detonation propagation through the U-bend. Curves 3 correspond to the results of Run 4 with SDT. Unfortunately, the experimental results of Run 3 with the ‘‘delayed’’ detonation initiation were not reproduced computationally. Nevertheless, curve 2 in Fig. 4 exhibit a ‘‘delayed’’ velocity jump of $(0.1\text{--}0.2)D_0$ at $L = 0.5$ m, which appeared not sufficient for detonation initiation.

Analysis of pressure histories in the detonation wave passing through the U-bend as a function of polar angle α measured from the entrance to the U-bend with the origin at the curvature center revealed some other important features. The pressure histories relevant to $\alpha = 0^\circ$ indicated that the initially planar detonation front exhibited pressure disturbances in the wake. The first evidence of the compression wave appeared on the pressure curve at the external wall. This compression propagated towards the internal wall. At $\alpha > 0^\circ$,

a pressure drop at the internal wall and symmetry surface was observed, whereas the pressure trace at the external wall showed the existence of the overdriven DW. At $\alpha = 67.5^\circ$, the shock pressure at the internal wall attained a nearly minimal value, which was consistent with the minimal shock velocity in Fig. 4a (curve 4). The pressure curve at the internal wall had a pressure hump characteristic of a SE (Fig. 3c). This SE resulted in an extremely high-pressure spike (above 8 MPa) at the internal wall at $\alpha = 112.5^\circ$. At the exit from the U-bend, the wave structure differed considerably from the planar incident wave at the U-bend entrance. Different portions of the lead front had different velocities and pressure amplitudes. The tails of the pressure traces exhibited regular oscillations. Large-scale unburned fuel pockets far behind the lead shock front were detected during detonation transition through the U-bend.

Figures 5a–c show calculated maximum pressure traces in the 2D channel at incident SW velocities of $0.73D_0$ (a), $0.75D_0$ (b), and $1.03D_0$ (c). Due to planar shock interaction with the walls of the U-bend, a transverse wave developed in the channel, which decayed at low incident SW velocity (Fig. 5a) and transformed to a detonation with a single transverse wave at high incident SW velocities (Figs. 5b and c). In Figs. 5b and c, the detonation structure is very similar, i.e., it does not depend on the way it is obtained. The detonation originated at a distance of about 1–2 tube

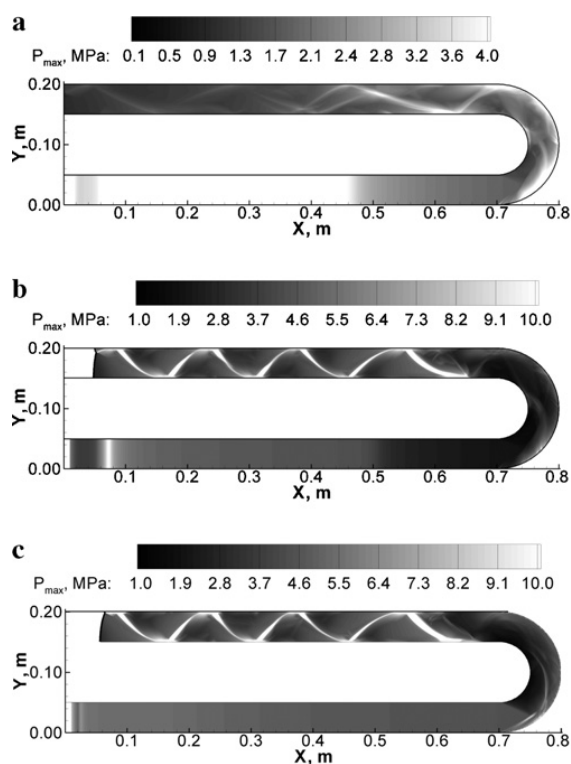


Fig. 5. Predicted maximum pressure traces at reactive shock and detonation transition through the U-bend. (a) $D = 0.73D_0$, (b) $D = 0.75D_0$, and (c) $D = 1.03D_0$.

diameters downstream from the U-bend exit. It took some distance (at least 5–6 tube diameters) for the DW to attain a sort of regular structure after exiting from the U-bend. Density disturbances in the wake of the propagating detonation also disappeared at a distance of about 5–6 tube diameters.

Figure 6 shows the comparison of calculations of SDT in tubes with U-bends of different curvature at identical initial conditions. Figures 6a and b correspond to the setups of Figs. 1a and b, respectively. In both computational runs, the primary SW was generated by a high-pressure domain in a lower left end of the tube with a pressure of 18 MPa and temperature of 298 K. The resulting SW entering the U-bend had a velocity of about 1000 m/s. It can be seen that a single-head detonation was initiated by such a SW in the tube with larger curvature (Fig. 6b), while SW deceleration was detected in the tube with smaller curvature (Fig. 6a). These results correspond well with the experimental findings.

Figure 7 shows the predicted effect of compression phase duration τ in the primary SW on SDT in the setup of Fig. 1a. The value of τ was defined as the time taken for the overpressure behind the SW to decrease by a factor of e with respect to its value at the shock front. The value of τ was varied by changing the length of a high-pressure initiation domain. Closed squares correspond to detonation initiation via SDT at a distance of up to 1.2 m behind the U-bend exit. Open squares correspond to “no-go” conditions for detonation initiation. Clearly, the SW with longer τ are more efficient for SDT in terms of the initial velocity.

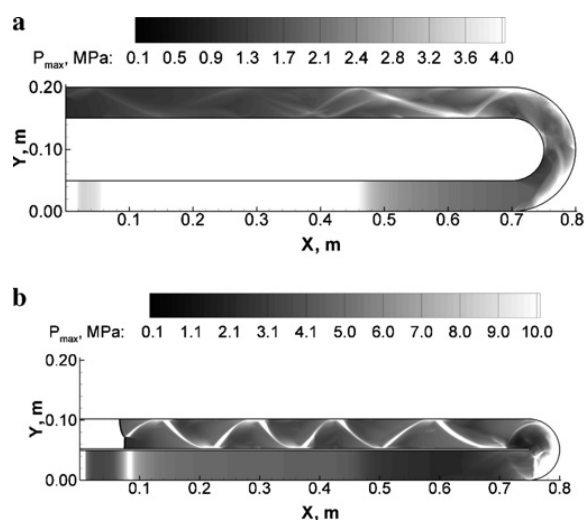


Fig. 6. Predicted fields of maximal pressure at identical conditions of SW generation in tubes with U-bends of different curvature: (a) no detonation, and (b) detonation.

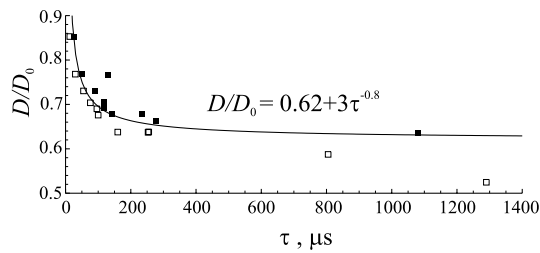


Fig. 7. Predicted effect of compression phase duration τ in the primary SW on SDT in the setup of Fig. 1a. Closed and open squares correspond to “go” and “no-go” conditions for detonation initiation downstream the U-bend. The curve is the approximation of the critical conditions for SDT.

6. Sensitivity analysis

To reveal the accompanying uncertainties in the computational studies, a sensitivity analysis was performed in terms of computational meshes and shock initiation techniques.

To reveal the effect of mesh “staircasing” at the curved boundaries, preliminary calculations of nonreactive and reactive SW and DW reflections from wedges were performed at different computational grids and compared with available experimental and computational data. The mesh “staircasing” affected considerably neither the flow pattern nor the ignition location behind the reflected reactive SW.

The results of calculations presented in Figs. 4–7 were proved to correspond well to similar calculations made with finer computational grids. Decreasing twice both the longitudinal and transverse mesh sizes resulted in insignificant (less than 0.5%) variation of the calculated SW and DW propagation velocities.

Figure 8 shows the effect of shock initiation technique on detonation dynamics in the U-bend. The DW was initiated by two separated high-pressure, high-temperature regions at the left end of the tube rather than by a single region. As a result of such nonplanar initiation, a cellular incident DW was obtained. The cell size in this DW was nearly equal to the channel

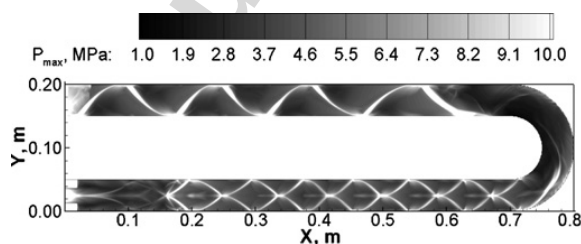


Fig. 8. Predicted maximum pressure traces at detonation transition through the U-bend: nonplanar initiation of the incident detonation.

width, which corresponded to the measured detonation cell size (about 50 mm) in the stoichiometric propane–air mixture at normal initial conditions [13]. Comparison of Figs. 8 and 5c indicates that the flow dynamics in the tube with U-bend was independent of the initiation technique. Based on the results of Fig. 8 it could be anticipated that in the long run the DW arising downstream from the U-bend might attain a single-cell structure similar to the incident DW structure.

7. Conclusions

Thus, the experimental results obtained in tubes with U-bends demonstrated a considerable effect of the U-bend on reactive SW and DW propagation. On the one hand, the U-bend promoted the shock-induced detonation initiation. On the other hand, the DW propagating through the U-bend was subjected to complete decay or to temporary attenuation with the velocity drop of up to 15–20%.

Two-dimensional numerical simulations of reactive SW and DW transition through the U-bends revealed salient features of relevant transient phenomena. Different portions of the lead shock front exhibited different behavior in the U-bends due to temporally and spatially shifted interaction with various compression and rarefaction waves and due to finite rate of chemical reaction. Localized secondary explosions were detected in the U-bends. In addition, large-scale unburned fuel pockets far behind the lead shock front were shown to form during shock and detonation transition through the U-bends. After exiting from the U-bend, shock or detonation decay, SDT, and reinitiation phenomena were observed depending on the incident wave velocity. In case of SDT and detonation reinitiation, a marginal detonation with a single transverse wave originated at a distance of 1–2 tube diameters downstream from the U-bends. It took about 5–6 tube diameters for this wave to attain a nearly regular structure. The important computational finding is possible variation of the detonation structure after passing the U-bend: a single-cell detonation may transform to a marginal detonation with a single transverse wave.

The U-bends of larger curvature and primary SW of longer compression phase duration were found to be more efficient for SDT in terms of the lower minimal SW velocity. However U-bends of larger curvature exhibited higher capability for suppressing the developed detonations. Thus the curvature of the U-bend and tube diameter are expected to be the most important governing parameters of the problem which determine the evolution of the initiating SW or a developed DW in such a system.

Acknowledgments

This work was partly supported by the US Office of Naval Research and International Science and Technology Center. Dr. Shamshin acknowledges the support of REC 011 “Fundamental investigation of matter under extreme conditions” and CRDF within the program “Basic Research and High Education.”

References

- [1] M.A. Nettleton, *Gaseous Detonations: Their Nature, Effects and Control*, Chapman and Hall, London—New York, 1987, 168 p.
- [2] S.M. Frolov, V.S. Aksenov, V.Ya. Basevich, *Doklady Phys. Chem.* 401 (1) (2005) 28–31.
- [3] S.M. Frolov, V.S. Aksenov, I.O. Shamshin, in: G. Roy, S. Frolov, A. Starik (Eds.), *Nonequilibrium Processes: Combustion and Detonation*, vol. 1, Torus Press, Moscow, 2005, p. 348.
- [4] S.M. Frolov, V.Ya. Basevich, V.S. Aksenov, in: G. Roy, A. Ghoniem (Eds.), *Proc. 17 ONR Propulsion Meeting*, MIT, Cambridge, MA, 2004, p. 181.
- [5] S.M. Frolov, V.S. Aksenov, V.Ya. Basevich, *Doklady Phys. Chem.* 402 (2) (2005) 93–95.
- [6] S.M. Frolov, *J. Propulsion Power* 22 (5) (2006).
- [7] A. Burcat, K. Scheller, A. Lifshitz, *Combust. Flame* 16 (3) (1971) 29.
- [8] A.A. Borisov, V.M. Zamanskii, V.V. Lissianskii, G.I. Skatchkov, K. Ya. Troshin, I.M. Baranov, *Chem. Phys. Rep.* 7 (5) (1988) 665.
- [9] V.M. Kovenya, N.N. Yanenko, *Splitting Method in Gasdynamic Problems*, Nauka, Novosibirsk, 1981.
- [10] V.P. Kolgan, *Uchenye Zapiski TsAGI* 3 (1972) 68.
- [11] V.V. Azatyan, A.M. Kogan, M.G. Neuhaus, A.I. Poroikova, E.N. Aleksandrov, *Kinet. Catalysis XVI* (3) (1975) 577–585.
- [12] A.A. Borisov, S.I. Sumskoii, I.O. Shamshin, P.V. Komissarov, M.A. Silakova, A.E. Mailkov, R.N. Elshin, *Chem. Phys. Rep.* 21 (5) (2002) 97.
- [13] R. Knystautas, C. Guirao, J. H. S. Lee, A. Sulmistras, in: J. Bowen, N. Manson, A. Oppenheim, R. Soloukhin (Eds.), *Dynamics of Shock Waves, Explosions, and Detonations*. Prog. Astron. Aeron. Ser., 94, 1984, p. 37.